

Trends and drivers in global surface ocean pH over the past three decades

S. K. Lauvset^{1,2}; N. Gruber³; P. Landschützer³; A. Olsen^{1,2,4}; J. Tjiputra.^{2,4}

¹Geophysical Institute, University of Bergen, Norway

²Bjerknes Center for Climate Research, Bergen, Norway

³Environmental Physics, Institute of Biogeochemistry and Pollutant Dynamics, ETH Zurich, Zürich, Switzerland.

⁴Uni Climate – Uni Research, Bergen, Norway

Correspondence to S. K. Lauvset (siv.lauvset@gfi.uib.no)

Abstract

We report global long-term trends in surface ocean pH using a new pH data set computed by combining fCO₂ observations from the Surface Ocean CO₂ Atlas (SOCAT) version 2 with surface alkalinity estimates based on temperature and salinity. Trends were determined over the periods 1981-2011 and 1991-2011 for a set of 17 biomes using a weighted linear least squares method. We observe significant decreases in surface ocean pH in ~70% of all biomes and a ~~global~~ mean rate of decrease of $-0.0018 \pm 0.0004 \text{ yr}^{-1}$ for 1991-2011. We are not able to calculate a global trend for 1981-2011 because too few biomes have enough data for this. In ~~two-thirds-of-half~~ the biomes, the rate of change is commensurate with the trends expected based on the assumption that the surface ocean pH change is only driven by the surface ocean ~~CO₂ carbon~~ chemistry remaining in a transient equilibrium with the increase in atmospheric CO₂. In the remaining biomes deviations from such equilibrium may reflect ~~changes in that~~ the trend of surface ocean fCO₂ ~~is not equal to that of the atmosphere~~, most notably in the equatorial Pacific Ocean, or changes in the oceanic buffer (Revelle) factor. We conclude that well-planned and long-term sustained observational networks are key to reliably document the ongoing and future changes in ocean carbon chemistry due to anthropogenic forcing.

1. Introduction

The concentration of atmospheric carbon dioxide (CO₂) is rapidly increasing due to the burning of fossil fuels, cement production, and land use changes (Le Quéré et al., 2014).

31 | This drives a net flux of CO₂ into the ocean, causing ~~its concentration of CO₂~~ the dissolved
32 | inorganic carbon (DIC) concentration to increase, which drives a decrease in pH and in the
33 | concentration of the carbonate ion (CO₃²⁻, Doney et al., 2009b; Zeebe and Wolf-Gladrow,
34 | 2001). These changes in the ocean inorganic carbon ~~chemistry-of the oceanic carbonate~~
35 | ~~system~~, collectively referred to as ocean acidification (Gattuso and Hansson, 2011), are a
36 | source of concern due to their potential impact on organisms, ecosystems and biogeochemical
37 | cycles (Doney et al., 2009a). Hereafter we refer to the inorganic carbon chemistry in the
38 | ocean as CO₂ chemistry. ~~But i~~In contrast to the surface ocean fugacity of carbon dioxide
39 | (fCO₂), for which many studies have analyzed the long-term trends, both regionally and
40 | globally (*e.g.* Fay and McKinley, 2013; Le Quéré, 2010; Lenton et al., 2012; Takahashi et al.,
41 | 2009b), only a handful of regional studies have so far been published on long-term pH trends
42 | (Bates, 2007; Dore et al., 2009; Gonzalez-Davila et al., 2007; Olafsson et al., 2010).

43 | The most extensive assessment to date is the one of Bates et al. (2014). They described
44 | changes in ocean ~~carbon cycle~~ CO₂ chemistry variables at seven, mostly tropical/sub-tropical,
45 | time-series stations, all of which have been occupied for at least two decades. Their analysis
46 | shows that while there are regional differences, these open ocean time-series show ~~remarkably~~
47 | relatively similar trends in ~~dissolved inorganic carbon (DIC)~~, fCO₂, and pH. At the tropical
48 | and subtropical open ocean stations (Bates, 2007; Dore et al., 2009; Gonzalez-Davila et al.,
49 | 2010) ocean pH is decreasing at a rate of $-0.0017 \pm 0.0002 \text{ yr}^{-1}$. At the high-latitude stations,
50 | however, a more variable picture emerges. While the pH trend in the Icelandic Sea follows the
51 | rate observed at the lower latitude stations, the trend in the Irminger Sea (Olafsson et al.,
52 | 2010) is nearly twice as large, *i.e.*, $-0.0026 \pm 0.0006 \text{ yr}^{-1}$. Thus, in a global analysis, we expect
53 | a complex spatial pattern of long-term trends, yet hitherto unknown.

54 | The absence of a global analysis of long-term trends is largely a consequence of the
55 | lack of direct surface ocean pH measurements, which is in sharp contrast to the situation for
56 | surface ocean fCO₂, for which data products contain several million observations (Bakker et
57 | al., 2014; Pfeil et al., 2013; Takahashi et al., 2009a). This limitation can be overcome by
58 | using computed pH, obtained by combining the very large data products of fCO₂ with
59 | estimates of surface alkalinity. Lauvset and Gruber (2014) demonstrated for the North
60 | Atlantic that this approach is able to produce rather accurate estimates of surface ocean pH.
61 | Takahashi et al. (2014) came to the same result globally. ~~This is largely because variations in~~
62 | ~~pH are mostly driven by variations in DIC following CO₂ uptake, and only to a lesser degree~~
63 | ~~by variations in alkalinity. Thus, uncertainties and errors in the alkalinity estimated from~~

64 | ~~salinity and temperature observations have only a limited effect on the uncertainties and error~~
65 | ~~of the computed pH (Lauvset and Gruber, 2014).~~

66 | Even though the use of pH computed from $f\text{CO}_2$ generates a global data set containing
67 | millions of pH observations, the resulting data are still sparse in time and space on a global
68 | scale, making the determination of global long-term trends challenging. For surface $p\text{CO}_2$ this
69 | challenge has historically been overcome by binning the data into a very coarse grid (order of
70 | 5° - 10° in latitude and longitude) by *e.g.* Lenton et al. (2012), Takahashi et al. (2002), and
71 | Takahashi et al. (2009b), but more recently Fay and McKinley (2013) proposed to aggregate
72 | the data into biomes. This type of aggregation is more likely to capture the correct long-term
73 | dynamics of a region, as one expects a biome to respond in a more coherent manner to
74 | perturbations than a region defined by a latitude/longitude range.

75 | Given the absence of a global observation-based analysis of pH trends, models have so
76 | far been the only source of information. The Norwegian Earth System Model (NorESM1-
77 | ME), as part of the Coupled Model Intercomparison Project phase 5 (CMIP5, Taylor et al.,
78 | 2012), simulates a global average pH decrease of -0.0017 yr^{-1} (1981-2011), which is largely
79 | commensurate with observations reported from the time series stations. A recent study using
80 | ten different CMIP5 models, including NorESM1-ME, showed that all models give similar
81 | global average pH trends—both in the historical and future scenarios (Bopp et al., 2013).

82 | This secular pH trend of -0.0017 yr^{-1} and the low spread between models is expected
83 | for an ocean where (i) the surface ocean $f\text{CO}_2$ follows that in the atmosphere due to the
84 | sufficiently rapid exchange of the excess CO_2 between the atmosphere and the surface ocean,
85 | and (ii) where the change in the buffer (Revelle) factor remains spatially uniform ~~and close to~~
86 | ~~constant~~, as the partial derivative $\partial[\text{H}^+]/\partial f\text{CO}_2$ is directly related to this quantity (Orr, 2011;
87 | Sarmiento and Gruber, 2006). A change in the buffer (Revelle) factor is expected as much of
88 | the CO_2 newly added to the surface ocean from the atmosphere will be titrated away by CO_3^{2-} ,
89 | causing a decrease in its concentration. This decreases the ability of the surface ocean to
90 | “buffer” the pH against further uptake of CO_2 , thus increasing the Revelle factor (Sarmiento
91 | and Gruber, 2006). However, regional variations in how the Revelle factor changes may
92 | occur. While the latter may be a good assumption for the global average, this may not be the
93 | case regionally and locally, where most of the impacts of ocean acidification will occur. Bates
94 | et al. (2014) show, for example, not only variations of the pH trends between the high- and
95 | low latitude time series secular trends, but also that the trends in Revelle factor are different, is
96 | increasing at all time series stations. This causes a decrease in the buffer capacity and hence a

97 ~~faster increase in surface ocean pH for a given increase in surface fCO₂ from the addition of~~
98 ~~CO₂. This trend in the Revelle factor is expected as much of the CO₂ newly added to the~~
99 ~~surface ocean from the atmosphere will be titrated away by CO₃²⁻ causing a decrease in its~~
100 ~~concentration. This decreases the ability of the surface ocean to “buffer” the pH against~~
101 ~~further uptake of CO₂, thus increasing the Revelle factor (Sarmiento and Gruber, 2006). But~~
102 ~~there are also indicating that other factors are influencing the Revelle factor.;~~ These factors
103 are mainly those processes that affect DIC and alkalinity, such as changes in ocean
104 productivity and calcification, while changes in temperature and salinity are of minor
105 importance (Sarmiento and Gruber, 2006).

106 Thus local and regional changes in the buffer (Revelle) factor are driven by the
107 changing, and spatially varying, ratio of DIC to alkalinity. Spatial changes in this ratio have
108 the potential to substantially decouple the pH trends from those of the surface ocean fCO₂
109 (Orr, 2011), potentially causing a more variable pattern in the pH trends. The complex spatial
110 variability, identified by Bates et al. (2014) and others (*e.g.* Tjiputra et al., 2014) supports this
111 hypothesis. This also shows that analyses of global pH trends, including the regional
112 distribution of changes and the dynamics of the changing ocean CO₂ system, are required for
113 a comprehensive understanding picture, including the regional distribution of changes and the
114 dynamics of the changing ocean carbon system. Global analyses are also necessary for the
115 validation of model results, for underpinning and interpreting response studies from organism
116 to ecosystem level, and for optimizing the planning of continued and future observational
117 networks.

118 Here we take advantage of the approach of Lauvset and Gruber (2014) to determine
119 global ocean pH trends, and their drivers, using pH data calculated from the more than 10
120 million observations of surface ocean fCO₂ that have been made available through the Surface
121 Ocean CO₂ Atlas (SOCAT) project (Bakker et al., 2014; Pfeil et al., 2013). ~~Although pH is~~
122 ~~the main parameter of our study fCO₂ has been carried through all of our analyses in order to~~
123 ~~determine how effects of carbonate chemistry variations causes the evolution of pH to differ~~
124 ~~from that expected from fCO₂ alone in many regions. Although pH is the main parameter of~~
125 interest, fCO₂ has been carried through all our analyses in order to determine how CO₂
126 chemistry causes the evolution of pH to differ from that expected from fCO₂ alone. Finally we
127 use the long term pH trends derived from a global earth system model, the NorESM1-ME, in
128 order to illustrate how important spatial variability is for the representativeness of our trend
129 results.

130

131 2. Data and Methods

132 We calculated pH in the surface ocean by a two-step calculation using observations of
133 fCO₂, sea surface temperature (SST), and sea surface salinity (SSS) from SOCAT version 2,
134 (Bakker et al., 2014). In the first step, alkalinity was calculated from SSS and SST using the
135 algorithms developed by Lee et al. (2006) and Nondal et al. (2009). The Nondal et al. (2009)
136 algorithms were developed specifically for the high-latitude (>60°N) Atlantic Ocean, and
137 were used only there. Whenever no measured SSS was available in the SOCATv2 data set the
138 climatological World Ocean Atlas SSS value (Antonov et al., 2010)—which is included in the
139 SOCATv2 data product—was used instead. The SOCAT SSS data have not been quality
140 controlled and might therefore be biased. Lauvset and Gruber (2014) showed that this
141 potential bias does not greatly affect the precision of the pH trends. It may affect the accuracy
142 of the calculation, but for our purpose of determining long-term trends, the accuracy (*i.e.* the
143 lack of bias in the data) is of less importance as long as the precision is good enough, and
144 assuming that any bias remains constant over time. In the second step, pH on the total scale at
145 *in situ* temperature was calculated from the estimated alkalinity and the observed fCO₂ using
146 CO2SYS (Lewis and Wallace, 1998). We used the K₁ and K₂ constants from Mehrbach et al.
147 (1973) refit by Dickson and Millero (1987), and the borate to salinity ratio from Uppström
148 (1974). Since we use CO2SYS this calculation also gives us dissolved inorganic carbon (DIC)
149 and all other variables of the ocean carbon chemistry system.

150 Quite a few of the data fall outside the valid ranges for input data for the Lee et al.
151 (2006) and Nondal et al. (2009) alkalinity algorithms and are lost in this step. There remains
152 7,381,013 data points of pH (and alkalinity) over the global ocean in the time period 1973-
153 2011. The fCO₂ trends have been estimated using only data points which have a calculated pH
154 value in order to avoid spurious differences when comparing these trends to those of pH. The
155 global calculation error (precision) for pH is 0.0032±0.0005, and the calculated pH compares
156 well to observed pH at crossover locations in the Atlantic Ocean (Lauvset and Gruber, 2014).
157 Before analysis the pH data were bin averaged into monthly 1°x1° bins, using no extrapolation
158 or interpolation of the data. The global data set was divided into the 17 ocean biomes,
159 (using mixed layer depth, sea surface temperature, and chlorophyll-a concentrations) and
160 named by Fay and McKinley (2014), as shown in Fig. Figure-1. Here, we only evaluate trends

161 | in the open ocean, ~~and d~~Data from coastal regions shallower than 250 m, based on the
162 | ETOPO2 bathymetry, and those with salinity <20 were removed.

163 | In each biome a least squares linear regression weighted with Tukey's bisquare
164 | method was used to determine the long-term pH trend. For the long-term trend determination
165 | we required each biome to have at least three observations in each decade (1981-1990, 1991-
166 | 2000, and 2001-2011). While this criterion was met in only 8 biomes for the period 1981-
167 | 2011, ~~all~~ 15 had sufficient data for the period 1991-2011. Both ordinary and weighted least
168 | squares regressions were carried out, but we chose a weighted least squares regression over an
169 | ordinary least squares regression since this is less sensitive to outliers in the data. This makes
170 | the statistics of the regression more robust, but generally this choice does not significantly
171 | affect the results presented here. All regression results are presented with the standard error of
172 | the slope (se), which represents its 68% confidence interval, and the root mean square error
173 | (RMSE). The RMSE is used as a measure of interannual variability.

174 | Before the regression analysis was carried out two corrections were applied to the
175 | data: deseasonalization and removal of spatial bias. The importance of these corrections,
176 | particularly in data sparse biomes such as those in the Southern Ocean, was recently
177 | highlighted by Fay et al. (2014). The seasonal cycle in the data was removed following
178 | Takahashi et al. (2009b), using the long-term average seasonal cycle as contained in our data
179 | for each biome ~~for this correction~~. However, we find that using the climatological seasonal
180 | cycle—calculated using the Takahashi pCO₂ climatology (Takahashi et al., 2009a)—~~does~~ not
181 | significantly affect the results. To correct for any spatial bias in the large scale biomes the
182 | difference between the climatological value in each 1°x1° bin and the biome mean
183 | climatological value was subtracted from the observed value in each 1°x1° bin. There is no
184 | difference between this method and simply subtracting the climatological value in each 1°x1°
185 | bin, but our approach retains the absolute values in each biome ~~mean values~~. It should be
186 | noted that the computed trends in some biomes are sensitive to which climatological data is
187 | used for the spatial bias correction: subtracting the climatological value vs. subtracting the
188 | long-term average in each 1°x1° bin. Mostly this is because in some 1°x1° bins, the long-term
189 | average is biased towards the last decade, which has significantly more data than earlier
190 | periods.

191 | A statistical test was performed to ~~test the necessity of these corrections~~ ensure that the
192 | ~~effects of these corrections do not corrupt our analysis~~: results after applying one or both
193 | corrections were compared to results after applying none using a one-way analysis of variance

194 (ANOVA, see *e.g.* Vijayvargiya, 2009). A statistically significant change in the slope and its
195 standard error was interpreted as making the correction(s) necessary. The deseasonalization
196 removes scatter in the data and leads to more robust regressions by reducing the standard
197 error of the slope in all biomes, but This correction does not significantly (p -value <0.05)
198 affect the long-term trend in any biome or time period, however. ~~The spatial bias correction~~
199 ~~has in most biomes no statistically significant impact on the long term trend~~ The spatial bias
200 correction has no statistically significant impact on the long term trend in most biomes, but
201 because it reduces the standard error and increases the r^2 in six biomes ~~does affect the trend in~~
202 ~~some biomes~~ we decided to keep it applied. The long-term pH trend is also much more
203 sensitive to this correction than the fCO₂ trend, mostly because the pH trend is very small and
204 thus more sensitive to any data correction.

205 The pH change expected from a certain change in fCO₂ ~~assuming everything else (*i.e.*~~
206 ~~alkalinity, DIC, SST, Revelle factor) remains constant~~ was calculated using $\Delta\text{pH}/\Delta\text{fCO}_2 =$
207 $\partial\text{pH}/\partial\text{fCO}_2$. The partial derivative was estimated in CO2SYS using 0.01 μatm increments in
208 fCO₂. Since both the fCO₂ and pH trends are inextricably coupled to DIC change, what we in
209 reality calculate here is the pH change incurred by a change in DIC equivalent to the given
210 fCO₂ trend when alkalinity, SST, and SSS remain constant. We used the same equation to
211 evaluate what global average fCO₂ change the global long-term trend in pH is consistent with,
212 but then using -0.001 incremental changes in pH. ~~Using such small increments allowed us to~~
213 ~~abide by the assumption of constant DIC and Revelle factor.~~

214 In each biome the long-term trend in pH was decomposed into the effects of changes
215 in SST, SSS, alkalinity, and DIC. First the impact of each of these drivers on the fCO₂ trend
216 was determined following Takahashi et al. (1993), equations 2-5, we then converted our
217 results to the impacts on [CO₂] and on [H⁺] following equation 1.5.87 in Zeebe and Wolf-
218 Gladrow (2001), and finally we determined the impact on pH. The DIC data and dissociation
219 constants required for these calculations were calculated in CO2SYS from the fCO₂ and
220 alkalinity pair in the same calculation that gave us pH.

221 ~~To test whether, and how the highly variable spatial and temporal coverage of the~~
222 ~~observational data affect the results we have~~ To test the effect of the highly variable spatial
223 and temporal coverage of the observational data on the results we have used the NorESM1-
224 ME Earth system model, which prognostically simulates the seawater CO₂-carbon chemistry.
225 A detailed description and evaluation of the model simulation is available in Tjiputra et al.
226 (2013). We examined the model simulation for the 1981-2011 period based on the CMIP5

227 historical and future RCP8.5 scenarios, where the atmospheric CO₂ concentration is used as
228 the boundary condition. We binned the model monthly output into the same 1°x1° bins and
229 used the same method to calculate and decompose the long-term trends in each biome as we
230 used for the observational data—including the two-step pH calculation described above. Two
231 sets of model trends were determined. For the first, we used the fully sampled model output,
232 referred to here as the ‘fully-sampled trend’. For the second set, we subsampled the model
233 output ~~following~~ according to the observational coverage, *i.e.* only data from monthly grid
234 cells corresponding to those where real observations have been obtained were used. The ‘sub-
235 sampled trend’ was then computed from these subsampled model data. The comparison of
236 these two informs us on how sensitive the calculated trends are to the variable data coverage.
237

238 3. Results and Discussion

239 3.1. Long-term trends in pH

240 We find statistically significant trends in 6 out of the 8 biomes with sufficient data for
241 the period 1981-2011, and for 13 out of the 15 biomes with sufficient data for the period
242 1991-2011 (~~Figure~~Fig. 1 with the numerical values in Table 1). As shown in ~~Figures~~Figs. 2-4,
243 the data coverage in each biome is generally very good after 1990, but often spotty prior to
244 this year. These figures also reveal a substantial amount of interannual variability around the
245 determined trends, with RMSE values of between 0.01 and 0.04 pH units— *i.e.*, roughly of
246 similar magnitude as the cumulative trend over the 20 to 30 years of analyses. No robust
247 analyses were possible for the North Pacific ice covered (NP-ICE) and North Atlantic ice
248 covered (NA-ICE) biomes, due to the lack of data (<20 data points) hence they are not further
249 discussed in the paper. Unfortunately, these are the Arctic biomes where the earliest impacts
250 of ocean acidification are expected (Steinacher et al., 2009).

251 The regions with sufficient data, but without statistically significant trends, *i.e.*, the
252 North Pacific subpolar seasonally stratified (NP-SPSS) biome for the period 1981-2011, and
253 the Southern Ocean subtropical seasonally stratified (SO-STSS) and ice covered (SO-ICE)
254 biomes for the period 1991-2011, are characterized by large RMSE and a substantial amount
255 of decadal variability, which is likely masking the long-term trends. In addition to these three
256 biomes where the trends are statistically indistinguishable from zero, the South Pacific
257 subtropical permanently stratified (SP-STPS) biome is likely biased by its low data density,

258 and will not be further discussed. This decision was corroborated~~was~~ by comparing the pH
259 trend in the fully-sampled model results with the sub-sampled model results (~~Figure~~Fig. 5):
260 the SP-STPS biome is the only one where the difference in these trends is statistically
261 significant at the 95% confidence level.

262 Since we are not able to calculate statistically significant trends in all 17 biomes we
263 are also unable to calculate a global average trend. For the period 1991-2011 only the Arctic
264 and parts of the Southern Ocean have no statistically significant results, and ~~T~~the area-
265 weighted~~global~~ average pH decrease of the remaining 13 biomes, including only statistically
266 significant trends (Table 1), is $-0.0018 \pm 0.0004 \text{ yr}^{-1}$ for the period 1991-2011. No global trend
267 can be computed ~~f~~For the period 1981-2011 ~~period~~, as the number of biomes with trend
268 estimates is ~~quite~~~~too~~ small, but almost all the Pacific Ocean biomes have results and the area-
269 weighted pH decrease~~trend in this period~~ is $-0.0019 \pm 0.0001 \text{ yr}^{-1}$ between 1981 and 2011.

270 Within the uncertainty limits the global 1991-2011 trend is comparable to the global trend in
271 the fully-sampled NorESM1-ME model results (-0.0017 yr^{-1}) and to the average trend of -
272 $0.0018 \pm 0.0003 \text{ yr}^{-1}$ over the seven time series evaluated by Bates et al. (2014). Assuming that
273 everything, including the Revelle factor, alkalinity, SST, and SSS remains constant, and that
274 the change in DIC and Revelle factor remains spatially uniform, this global average pH trend
275 corresponds to a rate of increase in surface ocean fCO_2 of $1.75 \pm 0.4 \mu\text{atm yr}^{-1}$, which is
276 roughly the rate of increase in atmospheric ~~p~~ fCO_2 . Regionally, however, the response of the
277 ocean CO₂-carbon system to the atmospheric forcing is more variable (~~Figure~~Fig. 1).

278 In the North Atlantic subpolar seasonally stratified (NA-SPSS) biome the observed pH
279 trend is $-0.0020 \pm 0.0004 \text{ yr}^{-1}$. This is right in between the trend observed at the Irminger Sea
280 time series ($-0.0026 \pm 0.0006 \text{ yr}^{-1}$) and that observed at the Iceland Sea time series (-
281 $0.0014 \pm 0.0005 \text{ yr}^{-1}$) (Bates et al., 2014). ~~But w~~Within the 68% confidence intervals, the NA-
282 SPSS pH trend is consistent with both of these local trends. In the North Atlantic subtropical
283 seasonally stratified (NA-STSS) biome there are no time series data to compare with, but its
284 trend of $-0.0018 \pm 0.0003 \text{ yr}^{-1}$ is consistent with a trend of $\sim -0.0020 \text{ yr}^{-1}$ observed in the
285 Rockall Trough by McGrath et al. (2012). In the North (NA-STPS) and South (SA-STPS)
286 Atlantic subtropical permanently stratified biomes the pH trend is the same, but the RMSE
287 values indicate larger interannual variability in the southern biome (Table 1). This is likely
288 caused by the inclusion of the Benguela upwelling region, but the full effect of this has not
289 been quantified for the SA-STPS or any other biome. The trend identified here for the NA-
290 STPS ($-0.0011 \pm 0.0002 \text{ yr}^{-1}$) is significantly lower than the trend observed at the Bermuda

291 Atlantic Time-series Study (BATS, Bates et al., 2014), of $-0.0017 \pm 0.0001 \text{ yr}^{-1}$. Unfortunately,
292 we have no time series data for comparison in the SA-STPS biome. In the Atlantic Ocean
293 equatorial region (A-EQU) the pH trend ($-0.0016 \pm 0.0003 \text{ yr}^{-1}$) is lower than that observed at
294 the Carbon Retention in A Colored Ocean (CARI~~A~~~~O~~~~C~~~~A~~~~O~~) time-series station of -
295 $0.0025 \pm 0.0004 \text{ yr}^{-1}$ (Bates et al., 2014), but this station is located at the very edge of the
296 biome in a more coastal setting and not ideal for comparison.

297 In the Pacific Ocean the RMSE around the fitted pH trends is generally larger than in
298 the Atlantic Ocean (Table 1), possibly reflecting the higher interannual variability of the
299 surface ~~CO₂-carbonate~~ system there (see *e.g.*, Landschützer et al. (2014) for pCO₂ variability).
300 In the North Pacific subtropical permanently stratified (NP-STPS) biome the pH trend of -
301 $0.0016 \pm 0.0002 \text{ yr}^{-1}$ is the same as that observed at the Hawaii Ocean Time-series (HOT, Bates
302 et al., 2014). The trends in the two equatorial Pacific Ocean biomes differ substantially. While
303 the western biome (WP-EQU) has a relatively weak trend ($-0.0010 \pm 0.0002 \text{ yr}^{-1}$), the eastern
304 (EP-EQU) biome has a much stronger pH trend than any other biome except the IO-STPS.
305 This could be related to the recent trend toward stronger and more prevalent La Niña
306 conditions in the eastern tropical Pacific leading to stronger upwelling, and higher surface
307 fCO₂ and lower pH in this region (Rödenbeck et al., 2014).

308 The Indian Ocean subtropical permanently stratified (IO-STPS) biome had a very
309 strong pH trend the past 30 years, only rivaled by that in the EP-EQU biome, as mentioned
310 above. There are not any time series stations in the Indian Ocean to compare with, but fCO₂
311 trends for the Indian Ocean computed by Metzl (2009) are considerably larger than what we
312 find: $2.11 \mu\text{atm yr}^{-1}$ vs $1.44 \pm 0.24 \mu\text{atm yr}^{-1}$. Hence there is no reason to believe that our
313 approach overestimates the pH trends here. It should be noted though that the trend identified
314 by Metzl (2009) is based on data in a considerably smaller region than the IO-STPS which
315 could account for some of the difference. In the Southern Ocean only the subpolar seasonally
316 stratified (SO-SPSS) biome has a statistically significant pH trend, which at -0.0020 ± 0.0002
317 yr^{-1} is comparable to that in the NA-SPSS biome. Further~~more~~, this trend is very similar to
318 that calculated for this region by Takahashi et al. (2014), although they~~had~~ used a different
319 method.

320 **3.2. Effects of changes in carbonate chemistry**

321 To first order, the pH trends are expected to represent the direct response to increasing
322 oceanic ~~DICCO₂~~, as is the case for the long-term trends in surface ocean fCO₂. In order to

323 | assess how our results compare ~~with~~against this expectation, we have calculated two expected
324 | pH rates of change: first the 1981-2011 change in pH resulting from a surface ocean fCO₂ rate
325 | of change equal to that in the atmosphere ($1.8 \pm 0.1 \mu\text{atm yr}^{-1}$) while keeping all other variables
326 | constant at their 1981 values; and second the change in pH that would be expected if the pH
327 | change mirrored the observed fCO₂ change in each biome provided that all other variables
328 | were kept at their 1981 values. The first expected pH change reflects how pH should change
329 | if the change in atmospheric CO₂ was the sole driver for the change in ocean pH. The second
330 | expected pH change reflects how pH should change if the oceanic fCO₂ changes were allowed
331 | to depart from the atmospheric ones but fCO₂ change remaining the only driver of pH change.
332 | ~~Given our method of calculation (Section 2), both expected pH estimates assumes constant~~
333 | ~~buffer (Revelle) factor.~~

334 | FigureFig. 6 shows both expected pH changes along with the observed pH change in
335 | each biome. Only the 13 biomes that have statistically significant pH trends for either 1981-
336 | 2011 or 1991-2011 (FigureFig. 1) are discussed further. When the atmospheric CO₂ increase
337 | is assumed to be the only driver for the pH changes, we find that in 75 of the 132 biomes the
338 | observed pH trends significantly differ from the expected pH change. This is due either to the
339 | uncertainty in the observed trends, to associated changes in the CO₂-carbonate chemistry, or
340 | to the surface ocean fCO₂ trends being significantly different from that in the atmosphere.
341 | However, the observed pH trends also significantly differ from the expected pH change
342 | calculated using the observed fCO₂ trend in 65 of the 132 biomes ~~also~~ (FigureFig. 6). Only 3
343 | of the 5 biomes are the same in both cases. Thus, the surface ocean fCO₂ trend not exactly
344 | mirroring the atmospheric cannot explain the discrepancy between expected and observed pH
345 | trends in most biomes. It may be an explanation in the equatorial Pacific biomes (EP-EQU
346 | and WP-EQU) where there is no discrepancy between observed and expected pH trends when
347 | the observed fCO₂ trend is used to calculate the expected pH change (FigureFig. 6), but a
348 | significant difference when an atmospheric rate of change is assumed.

349 | The observed pH trend is more often smaller than that expected for the ocean
350 | mirroring the atmospheric fCO₂ change than vice versa. Only the EP-EQU and IO-STPS
351 | biomes ~~has~~ have an observed pH changes larger than those expected (FigureFig. 6). Our
352 | hypothesis is that the differences between the observed and expected pH trends are caused by
353 | changes in the spatial variations in the ratio of DIC to alkalinity, which leads to spatial
354 | changes in the buffer (Revelle) factor. In the biomes where the observed trend differs from the
355 | expected trend there are indications which point to such changes. When the difference is

356 ~~negative (*i.e.*, the observed trend is smaller than the expected), the decrease in Revelle factor,~~
357 ~~*e.g.*, is stronger the larger the difference. in carbonate chemistry, *e.g.* that the temporal trends~~
358 ~~in both $\partial[\text{H}^+]/\partial\text{pCO}_2$ (Gattuso and Hansson, 2011) and Revelle factor are consistent with the~~
359 ~~differences between expected and observed pH change.~~ However, given the combined
360 calculation errors, generally high level of noise in our data, and relatively few data points,
361 only some of these indications are statistically significant. Further analysis of these spatial
362 patterns needs to be undertaken using independent pH data, preferably direct measurements in
363 order to quantify any possible biases in the results due to our pH being a calculated variable.
364 A combination of SOCAT data with repeat hydrography and time-series data would be ideal
365 but this is outside the scope of this study.

366 **3.3. Major driving forces behind the observed pH and trends**

367 The decomposition of the fCO_2 and pH trends confirms (~~Figures~~[Figs. 8-107-9](#)) that in
368 all biomes the long-term increase in DIC is by far the dominant driver for the long-term pH
369 changes. ~~Thus, k~~Knowledge about the changes in ocean DIC therefore is the most important
370 in understanding—and predicting—changes in ocean pH (Table 2). This is not unexpected
371 since the open ocean is in—or very close to—chemical equilibrium with the atmosphere
372 (Lauvset and Gruber, 2014). Thus the surface ocean is taking up CO_2 from the atmosphere in
373 order to re-establish a chemical equilibrium, leading to a corresponding increase in ~~p~~ fCO_2 and
374 DIC. It must be noted that since we do not have measurements of alkalinity this parameter is
375 calculated from SST and SSS, and the relatively large uncertainties in these calculations may
376 add a degree of uncertainty to the decomposition. Due to a lack of independent data this is not
377 further evaluated in this study.

378 In the Atlantic Ocean biomes the second most important driver is SST (~~Figure~~[Fig. 78](#)),
379 which mostly has a positive change and therefore has limited the DIC increase required to
380 maintain an fCO_2 growth rate similar to that in the atmosphere. SST is the second most
381 important driver also in the Pacific Ocean biomes (~~except in the NP-SPSS, Figure~~[Fig. 89](#)), but
382 here SST decreased in many biomes leading to an enhanced increase in DIC through CO_2
383 uptake from the atmosphere. In the Southern Ocean biomes alkalinity changes have a
384 significant impact on the trends (~~Figure~~[Fig. 910](#)), which also modulates the DIC changes.
385 Decreasing alkalinity over time increases fCO_2 so that the DIC change required to maintain a
386 sea surface fCO_2 growth rate similar to the atmospheric is reduced.

387 In most biomes there is a residual between the sum of the four components and the
388 observed trend (~~Figure~~[Fig. 107](#)). Lenton et al. (2012) performed a similar analysis and
389 attributed such residuals to the use of a spatial mean Revelle factor, the approximations
390 underlying the Takahashi et al. (1993) equations, and the assumption of linear trends in all
391 variables. We tested whether variable data coverage is also an important contributor to this
392 residual by subsampling the NorESM1-ME simulated pH data and comparing the resulting
393 1981-2011 decomposition with the decomposition determined using the full model output.
394 ~~Figure~~[Fig. 107](#) illustrates that in most biomes there are similar residuals between the sum of
395 the four components and the actual trends in the sub-sampled and fully-sampled model fields
396 as well. We can, therefore, find no evidence to show that poor data coverage is of major
397 importance in determining what drives the change in surface ocean pH.

398 3.4. Recent changes in the Southern Ocean biomes

399 ~~In contrast to the majority of the global ocean biomes, trends within the SO-STSS and~~
400 ~~SO-ICE biomes do not appear statistically significant over the past two decades (Table 1).~~
401 ~~This can be linked to strong interannual and decadal variations (Fig. 3). While this study~~
402 ~~generally does not have statistically significant results in the Southern Ocean our results do~~
403 ~~indicate significant decadal variations in the trends (Table 1).~~ This is consistent with the
404 changing fCO₂ trends [revealed](#) in a recent study by Fay et al. (2014) as well as previous
405 findings of a change in the CO₂ sink in this region (*e.g.* Fay and McKinley, 2013;
406 Landschützer et al., 2014). In order to investigate these recent [changes in the](#) trend ~~changes~~ in
407 the Southern Ocean, we also decompose the 2001-2011 trends in the Southern Ocean biomes
408 (Table 3).

409 ~~In the SO-STSS biome there is no significant change in pH over the 30 year period,~~
410 ~~but from Fig. 3 it is seen that there is a decrease until ~2000 and then an increase over the last~~
411 ~~decade. Over the last decade (Table 3) we find that the contributions of the individual~~
412 ~~parameters to the overall trend in pH are amplified. Temperature and DIC changes remain the~~
413 ~~strongest drivers, and of these the forcing from DIC has increased strongest over the last~~
414 ~~decade. We hence conclude that the increase in pH over the past decade in the SO-STSS~~
415 ~~biome is due to the decreasing DIC concentrations dominating over the thermally induced~~
416 ~~reduction in pH. In the SO-STSS biome we find no change in what drives the pH trend for~~
417 ~~this decade compared to the longer period. However, the change in the observed pH trend~~
418 ~~(Table 3) appears to be dominated by the change in DIC as this is approximately four times~~

419 ~~larger (more negative) for the period 2001–2011 than for the period 1981–2011, and therefore~~
420 ~~likely dominates over the thermally induced reduction of the pH trends.~~

421 In the SO-SPSS biome the pH trend appears to become less steep over the last decade
422 (Fig. 3), which is consistent with the well-documented trend changes in fCO₂. In ~~this~~ SO-
423 SPSS biome we find ~~an increase in the~~ less negative DIC driven pH trend ~~within~~ the period
424 2001–2011 compared to the period 1981–2011, ~~and since the~~ indicating a reduced increasing
425 trend in DIC ~~component is negative this over this decade.~~ This supports the conclusion drawn
426 by Fay and McKinley (2013) that a reduction in vertical DIC ~~supply~~ support causes ~~the~~
427 weakening of both fCO₂ and pH trends in this region. In the SO-ICE biome the sign of the
428 non-thermal drivers appears to change within the last decade, potentially driven by the recent
429 Antarctic ice melt and ice-sheet melting driven iron fertilization (Death et al., 2014).

430 3.5. Spatial variability

431 In both the observations and the sub-sampled model results we see significant regional
432 differences in the pH trends (~~Figure~~ Fig. 5). Note that the actual simulated pH trends in each
433 biome are not directly comparable with the observed trends since the model is a coupled
434 climate model, which simulates its own internal climate variability. We therefore compare the
435 fully sampled and the sub-sampled model results, and the fully sampled model results show
436 much more uniform pH trends (~~Figure~~ Fig. 5). While these differences are mostly statistically
437 indistinguishable within the uncertainties, it highlights the need for careful consideration of
438 representativeness when comparing model-derived future changes and trends based on data.
439 ~~Fig. Figure-5~~ shows that in the ~~IO-STPS and WP-EQU~~ SO-SPSS, EP-EQU, AEQU, and NP-
440 STPS biomes the sub-sampled trend is within ± 0.0001 of the fully-sampled pH trends, and an
441 ANOVA analysis shows that only in the SP-STPS biome are the two model trends
442 significantly different. Thus the trends based on the existing observational coverage are
443 overall representative of the respective biomes, and it is unlikely ~~that there are to be~~ major
444 biases in our results due to low data density. However, the uncertainties in the long-term pH
445 trend estimates remain ~~too~~ large, both in observations and ~~the~~ model (~~Figure~~ Fig. 5) and this
446 prohibits a mechanistic understanding the observed changes in most biomes. Improved
447 sampling strategies are necessary to reduce these uncertainties and thereby improve our
448 understanding of surface ocean CO₂-carbon chemistry changes today and in the future.

449 This highlights the importance of both maintaining the observational networks already
450 in place—like the voluntary observing ship (VOS) network in the North Atlantic (Watson et

451 al., 2009)—and instigating new ones in less well-covered ocean regions. Of particular
452 importance is improved data coverage in the Southern Pacific Ocean (SP-STPS) where the
453 data density as of today it too low for a robust analysis of long term pH trends.
454

455 4. Conclusions

456 Global surface ocean pH changes over the past 30 years cannot be calculated as there
457 are too few data in many biomes. For the past twenty years on the other hand, we find that
458 the surface ocean pH has decreased by on average $0.0018 \pm 0.0004 \text{ yr}^{-1}$, excluding the Arctic
459 and high-latitude Southern Ocean~~has decreased over the past 20 years by $-0.0018 \pm 0.0004 \text{ yr}^{-1}$.~~

460 There are however large regional variations with trends ranging from -0.0024 yr^{-1} in the
461 Indian Ocean (IO-STPS) biome to no significant change in the polar Southern Ocean (SO-
462 ICE) biome. Our estimated global trend is ~~very~~ comparable to the trends found at time-series
463 stations and to the global average trends in the ~~CMIP5 NorESM1-ME~~ models. In all biomes,
464 the pH trend is predominantly driven by changes in DIC, implying that the surface ocean pH
465 decline is a direct response to the increasing uptake of atmospheric CO_2 . Despite this, the
466 fCO_2 and pH trends do not exactly mirror each other, which is potentially linked to trends in
467 the surface ocean buffer (Revelle) factor over the past decades. In some biomes this leads to
468 smaller pH changes than expected from the fCO_2 change, while in others regions, the pH
469 changes are larger than expected. Thus, knowledge of both the changing ocean DIC and the
470 changing ocean buffer (Revelle) factor is important for understanding and accurately
471 determining the changing ocean pH.

472 There are regional differences in the pH trends. It is likely that these are caused by
473 spatial heterogeneity in the concurrent changes in buffer (Revelle) factor, while spatial
474 heterogeneity in the surface ocean fCO_2 trends seems to have only a minor effect. Our
475 comparison between fully-sampled model and sub-sampled output from the NorESM1-ME
476 model indicates that variable data coverage only presents a major problem in the South
477 Pacific. This nicely highlights the overall success of the scientific community in creating
478 observational networks that reduce data coverage issues. The many scientific studies arising
479 from this effort—among many others the recent publications by Nakaoka et al. (2013),
480 Landschützer et al. (2013), Landschützer et al. (2014), and Schuster et al. (2013)—show that
481 we have come a long way in understanding how ocean CO_2 -carbon chemistry is evolving in a
482 world perturbed by fossil fuel emissions. The uncertainties in the trends presented here are,

483 however, substantial and this largely prevents a more thorough understanding of current
484 changes. Filling the remaining gaps in our surface ocean data, ~~and quantifying spatial patterns~~
485 ~~in the carbon chemistry parameters~~, is, therefore, still of great importance, ~~in order to~~
486 ~~accurately assess the open ocean carbon chemistry changes.~~
487

488 **Acknowledgements**

489 The work of S. K. Lauvset was funded by the Norwegian Research Council through the
490 project DECApH (214513/F20). Are Olsen acknowledge funding from the Centre for
491 Climate Dynamics at the Bjerknes Centre for Climate Research, and the Norwegian Research
492 Council project SNACS (229756). N. Gruber and P. Landschützer acknowledge funding
493 from the ETH and the EU FP7 projects CARBOCHANGE (264879) and GEOCARBON
494 (283080). J. Tjiputra acknowledges the Centre for Climate Dynamics project
495 BIOFEEDBACK.
496

497 **References**

498 Antonov, J., Seidov, D., Boyer, T., Locarnini, R., Mishonov, A., Garcia, H., Baranova, O.,
499 Zweng, M., and Johnson, D.: World Ocean Atlas 2009, vol. 2, Salinity, edited by S.
500 Levitus, 184 pp, US Gov. Print. Off., Washington, DC, 2010. 2010.

501 Bakker, D. C. E., Pfeil, B., Smith, K., Hankin, S., Olsen, A., Alin, S. R., Cosca, C., Harasawa,
502 S., Kozyr, A., Nojiri, Y., O'Brien, K. M., Schuster, U., Telszewski, M., Tilbrook, B.,
503 Wada, C., Akl, J., Barbero, L., Bates, N. R., Boutin, J., Bozec, Y., Cai, W. J., Castle, R.
504 D., Chavez, F. P., Chen, L., Chierici, M., Currie, K., de Baar, H. J. W., Evans, W.,
505 Feely, R. A., Fransson, A., Gao, Z., Hales, B., Hardman-Mountford, N. J., Hoppema,
506 M., Huang, W. J., Hunt, C. W., Huss, B., Ichikawa, T., Johannessen, T., Jones, E. M.,
507 Jones, S. D., Jutterström, S., Kitidis, V., Körtzinger, A., Landschützer, P., Lauvset, S.
508 K., Lefèvre, N., Manke, A. B., Mathis, J. T., Merlivat, L., Metzl, N., Murata, A.,
509 Newberger, T., Omar, A. M., Ono, T., Park, G. H., Paterson, K., Pierrot, D., Ríos, A. F.,
510 Sabine, C. L., Saito, S., Salisbury, J., Sarma, V. V. S. S., Schlitzer, R., Sieger, R.,
511 Skjelvan, I., Steinhoff, T., Sullivan, K. F., Sun, H., Sutton, A. J., Suzuki, T., Sweeney,
512 C., Takahashi, T., Tjiputra, J., Tsurushima, N., van Heuven, S. M. A. C., Vandemark,
513 D., Vlahos, P., Wallace, D. W. R., Wanninkhof, R., and Watson, A. J.: An update to the
514 Surface Ocean CO₂ Atlas (SOCAT version 2), Earth Syst. Sci. Data, 6, 69-90, 2014.

515 Bates, N. R.: Interannual variability of the oceanic CO₂ sink in the subtropical gyre of the
516 North Atlantic Ocean over the last 2 decades, *J. Geophys. Res.-Oceans*, 112, 26, 2007.

517 Bates, N. R., Astor, Y. M., Church, M. J., Currie, K., Dore, J. E., Gonzalez-Davila, M.,
518 Lorenzoni, L., Muller-Karger, F., Olafsson, J., and Magdalena Santana-Casiano, J.: A
519 Time-Series View of Changing Surface Ocean Chemistry Due to Ocean Uptake of
520 Anthropogenic CO₂ and Ocean Acidification, *Oceanography*, 27, 126-141, 2014.

521 Bopp, L., Resplandy, L., Orr, J. C., Doney, S. C., Dunne, J. P., Gehlen, M., Halloran, P.,
522 Heinze, C., Ilyina, T., Seferian, R., Tjiputra, J., and Vichi, M.: Multiple stressors of
523 ocean ecosystems in the 21st century: projections with CMIP5 models, *Biogeosciences*,
524 10, 6225-6245, 2013.

525 Dickson, A.G. and Millero, F.J., 1987. A comparison of the equilibrium-constants for the
526 dissociation of carbonic-acid in seawater media. *Deep-Sea Research Part a-*
527 *Oceanographic Research Papers*, 34(10): 1733-1743.

528 Death, R., Wadham, J. L., Monteiro, F., Le Brocq, A. M., Tranter, M., Ridgwell, A.,
529 Dutkiewicz, S., and Raiswell, R.: Antarctic ice sheet fertilises the Southern Ocean,
530 *Biogeosciences*, 11, 2635-2643, 2014.

531 Doney, S. C., Balch, W. M., Fabry, V. J., and Feely, R. A.: Ocean Acidification: A critical
532 emerging problem for the ocean sciences, *Oceanography*, 22, 16-25, 2009a.

533 Doney, S. C., Fabry, V. J., Feely, R. A., and Kleypas, J. A.: Ocean Acidification: The Other
534 CO₂ Problem, *Annual Review of Marine Science*, 1, 169-192, 2009b.

535 Dore, J. E., Lukas, R., Sadler, D. W., Church, M. J., and Karl, D. M.: Physical and
536 biogeochemical modulation of ocean acidification in the central North Pacific,
537 *Proceedings of the National Academy of Sciences*, 106, 12235-12240, 2009.

538 Fay, A. R. and McKinley, G. A.: Global trends in surface ocean pCO₂ from in situ data,
539 *Global Biogeochemical Cycles*, 27, 541-557, 2013.

540 Fay, A. R. and McKinley, G. A.: Global Ocean Biomes: Mean and time-varying maps
541 (NetCDF 7.8 MB), doi:10.1594/PANGAEA.828650, 2014, Supplement to: Fay, A. R.
542 and McKinley, G. A.: Global open-ocean biomes: mean and temporal variability, *Earth*
543 *Syst. Sci. Data*, 6, 273–284, doi: 10.5194/essd-6-273-2014, 2014.

544 Fay, A. R., McKinley, G. A., and Lovenduski, N. S.: Southern Ocean carbon trends:
545 sensitivity to methods, *Geophys. Res. Lett.*, 41, doi: 10.1002/2014GL061324, online
546 first, 2014.

547 Gattuso, J.-P. and Hansson, L.: Ocean Acidification, Oxford University Press, New York,
548 2011

549 Gonzalez-Davila, M., Santana-Casiano, J. M., and Gonzalez-Davila, E. F.: Interannual
550 variability of the upper ocean carbon cycle in the northeast Atlantic Ocean, *Geophysical*
551 *Research Letters*, 34, 2007.

552 Gonzalez-Davila, M., Santana-Casiano, J. M., Rueda, M. J., and Llinas, O.: The water column
553 distribution of carbonate system variables at the ESTOC site from 1995 to 2004,
554 *Biogeosciences*, 7, 3067-3081, 2010.

555 Landschützer, P., Gruber, N., Bakker, D. C. E., and Schuster, U.: Recent variability of the
556 global ocean carbon sink, *Global Biogeochemical Cycles*, doi: 10.1002/2014GB004853,
557 2014. 2014GB004853, 2014.

558 Landschützer, P., Gruber, N., Bakker, D. C. E., Schuster, U., Nakaoka, S., Payne, M. R.,
559 Sasse, T. P., and Zeng, J.: A neural network-based estimate of the seasonal to inter-
560 annual variability of the Atlantic Ocean carbon sink, *Biogeosciences*, 10, 7793-7815,
561 2013.

562 Lauvset, S. K. and Gruber, N.: Long-term trends in surface ocean pH in the North Atlantic,
563 *Marine Chemistry*, 162, 71-76, 2014.

564 Lewis, E. and Wallace, D.W.R.: Program developed for CO₂ system calculations,
565 ORNL/CDIAC-105. Carbon Dioxide Information Analysis Center, Oak Ridge National
566 Laboratory, U.S. Department of Energy, Oak Ridge, Tennessee, 1998.

567 Le Quéré, C.: Trends in the land and ocean carbon uptake, *Current Opinion in Environmental*
568 *Sustainability*, 2, 219-224, 2010.

569 Le Quéré, C., Peters, G. P., Andres, R. J., Andrew, R. M., Boden, T. A., Ciais, P.,
570 Friedlingstein, P., Houghton, R. A., Marland, G., Moriarty, R., Sitch, S., Tans, P.,
571 Arneeth, A., Arvanitis, A., Bakker, D. C. E., Bopp, L., Canadell, J. G., Chini, L. P.,
572 Doney, S. C., Harper, A., Harris, I., House, J. I., Jain, A. K., Jones, S. D., Kato, E.,
573 Keeling, R. F., Klein Goldewijk, K., Körtzinger, A., Koven, C., Lefèvre, N., Maignan,
574 F., Omar, A., Ono, T., Park, G. H., Pfeil, B., Poulter, B., Raupach, M. R., Regnier, P.,
575 Rödenbeck, C., Saito, S., Schwinger, J., Segschneider, J., Stocker, B. D., Takahashi, T.,
576 Tilbrook, B., van Heuven, S., Viovy, N., Wanninkhof, R., Wiltshire, A., and Zaehle, S.:
577 Global carbon budget 2013, *Earth Syst. Sci. Data*, 6, 235-263, 2014.

578 Lee, K., Tong, L. T., Millero, F. J., Sabine, C. L., Dickson, A. G., Goyet, C., Park, G.-H.,
579 Wanninkhof, R., Feely, R. A., and Key, R. M.: Global relationships of total alkalinity

580 with salinity and temperature in surface waters of the world's oceans, *Geophysical*
581 *Research Letters*, 33, L19605, 2006.

582 Lenton, A., Metzl, N., Takahashi, T., Kuchinke, M., Matear, R. J., Roy, T., Sutherland, S. C.,
583 Sweeney, C., and Tilbrook, B.: The observed evolution of oceanic pCO₂ and its drivers
584 over the last two decades, *Global Biogeochem. Cycles*, 26, GB2021, 2012.

585 McGrath, T., Kivimae, C., Tanhua, T., Cave, R. R., and McGovern, E.: Inorganic carbon and
586 pH levels in the Rockall Trough 1991-2010, *Deep-Sea Research Part I-Oceanographic*
587 *Research Papers*, 68, 79-91, 2012.

588 Mehrbach, C., Culberso, Ch, Hawley, J.E. and Pytkowic, Rm, 1973. Measurement of apparent
589 dissociation-constants of carbonic-acid in seawater at atmospheric-pressure. *Limnology*
590 *and Oceanography*, 18(6): 897-907.

591 Metzl, N.: Decadal increase of oceanic carbon dioxide in Southern Indian Ocean surface
592 waters (1991–2007), *Deep Sea Research Part II: Topical Studies in Oceanography*, 56,
593 607-619, 2009.

594 Nakaoka, S., Telszewski, M., Nojiri, Y., Yasunaka, S., Miyazaki, C., Mukai, H., and Usui, N.:
595 Estimating temporal and spatial variation of ocean surface pCO₂ in the North Pacific
596 using a self-organizing map neural network technique, *Biogeosciences*, 10, 6093-6106,
597 2013.

598 Nondal, G., Bellerby, R. G. J., Olsen, A., Johannessen, T., and Olafsson, J.: Optimal
599 evaluation of the surface ocean CO₂ system in the northern North Atlantic using data
600 from voluntary observing ships, *Limnol. Oceanogr. Meth.*, 7, 109-118, 2009.

601 Olafsson, J., Olafsdottir, S. R., Benoit-Cattin, A., and Takahashi, T.: The Irminger Sea and the
602 Iceland Sea time series measurements of sea water carbon and nutrient chemistry 1983–
603 2008, *Earth Syst. Sci. Data*, 2, 99-104, 2010.

604 Orr, J.: Recent and future changes in ocean carbonate chemistry. In: *Ocean acidification*,
605 Gattuso, J.-P. and Hansson, L. (Eds.), Oxford University Press, New York, 41-66, 2011.

606 Pfeil, B., Olsen, A., Bakker, D. C. E., Hankin, S., Koyuk, H., Kozyr, A., Malczyk, J., Manke,
607 A., Metzl, N., Sabine, C. L., Akl, J., Alin, S. R., Bates, N., Bellerby, R. G. J., Borges,
608 A., Boutin, J., Brown, P. J., Cai, W. J., Chavez, F. P., Chen, A., Cosca, C., Fassbender,
609 A. J., Feely, R. A., González-Dávila, M., Goyet, C., Hales, B., Hardman-Mountford, N.,
610 Heinze, C., Hood, M., Hoppema, M., Hunt, C. W., Hydes, D., Ishii, M., Johannessen,
611 T., Jones, S. D., Key, R. M., Körtzinger, A., Landschützer, P., Lauvset, S. K., Lefèvre,
612 N., Lenton, A., Laurantou, A., Merlivat, L., Midorikawa, T., Mintrop, L., Miyazaki, C.,

613 Murata, A., Nakadate, A., Nakano, Y., Nakaoka, S., Nojiri, Y., Omar, A. M., Padin, X.
614 A., Park, G. H., Paterson, K., Perez, F. F., Pierrot, D., Poisson, A., Ríos, A. F., Santana-
615 Casiano, J. M., Salisbury, J., Sarma, V. V. S. S., Schlitzer, R., Schneider, B., Schuster,
616 U., Sieger, R., Skjelvan, I., Steinhoff, T., Suzuki, T., Takahashi, T., Tedesco, K.,
617 Telszewski, M., Thomas, H., Tilbrook, B., Tjiputra, J., Vandemark, D., Veness, T.,
618 Wanninkhof, R., Watson, A. J., Weiss, R., Wong, C. S., and Yoshikawa-Inoue, H.: A
619 uniform, quality controlled Surface Ocean CO₂ Atlas (SOCAT), *Earth Syst. Sci. Data*,
620 5, 125-143, 2013.

621 Rödenbeck, C., Bakker, D. C. E., Metzl, N., Olsen, A., Sabine, C., Cassar, N., Reum, F.,
622 Keeling, R. F., and Heimann, M.: Interannual sea–air CO₂ flux variability from an
623 observation-driven ocean mixed-layer scheme, *Biogeosciences*, 11, 4599–4613,
624 doi:10.5194/bg-11-4599-2014, 2014.

625 Sarmiento, J. L. and Gruber, N.: *Ocean biogeochemical dynamics*, Princeton University Press,
626 Princeton, N.J., 2006.

627 Schuster, U., McKinley, G. A., Bates, N., Chevallier, F., Doney, S. C., Fay, A. R., González-
628 Dávila, M., Gruber, N., Jones, S., Krijnen, J., Landschützer, P., Lefèvre, N., Manizza,
629 M., Mathis, J., Metzl, N., Olsen, A., Rios, A. F., Rödenbeck, C., Santana-Casiano, J.
630 M., Takahashi, T., Wanninkhof, R., and Watson, A. J.: An assessment of the Atlantic
631 and Arctic sea–air CO₂ fluxes, 1990–2009, *Biogeosciences*, 10, 607-627, 2013.

632 Steinacher, M., Joos, F., Froelicher, T. L., Plattner, G. K., and Doney, S. C.: Imminent ocean
633 acidification in the Arctic projected with the NCAR global coupled carbon cycle-
634 climate model, *Biogeosciences*, 6, 515-533, 2009.

635 Takahashi, T., Olafsson, J., Goddard, J. G., Chipman, D. W., and Sutherland, S. C.: Seasonal-
636 Variation of CO₂ and Nutrients in the High-Latitude Surface Oceans - A Comparative
637 Study, *Global Biogeochemical Cycles*, 7, 843-878, 1993.

638 Takahashi, T., Sutherland, S. C., Chipman, D. W., Goddard, J. G., Ho, C., Newberger, T.,
639 Sweeney, C., and Munro, D. R.: Climatological distributions of pH, pCO₂, total CO₂,
640 alkalinity, and CaCO₃ saturation in the global surface ocean, and temporal changes at
641 selected locations, *Marine Chemistry*, 164, 95-125, 2014.

642 Takahashi, T., Sutherland, S. C., and Kozyr, A.: Global Ocean Surface Water Partial Pressure
643 of CO₂ Database: Measurements Performed During 1968-2008 (Version 2008). . In:
644 ORNL/CDIAC-152, NDP-088r, Carbon Dioxide Information Analysis Center, Oak
645 Ridge National Laboratory, U.S. Department of Energy, Oak Ridge, Tennessee, 2009a.

646 Takahashi, T., Sutherland, S. C., Sweeney, C., Poisson, A., Metzl, N., Tilbrook, B., Bates, N.
647 R., Wanninkhof, R., Feely, R. A., Sabine, C. L., Olafsson, J., and Nojiri, Y.: Global sea-
648 air CO₂ flux based on climatological surface ocean pCO₂, and seasonal biological and
649 temperature effects, *Deep-Sea Research II*, 49, 1601-1622, 2002.

650 Takahashi, T., Sutherland, S. C., Wanninkhof, R., Sweeney, C., Feely, R. A., Chipman, D.
651 W., Hales, B., Friederich, G., Chavez, F., Sabine, C., Watson, A., Bakker, D. C. E.,
652 Schuster, U., Metzl, N., Yoshikawa-Inoue, H., Ishii, M., Midorikawa, T., Nojiri, Y.,
653 Körtzinger, A., Steinhoff, T., Hoppema, M., Olafsson, J., Arnarson, T. S., Tilbrook, B.,
654 Johannessen, T., Olsen, A., Bellerby, R., Wong, C. S., Delille, B., Bates, N. R., and de
655 Baar, H. J. W.: Climatological mean and decadal change in surface ocean pCO₂, and
656 net sea-air CO₂ flux over the global oceans, *Deep-Sea Research Part II - Topical
657 Studies in Oceanography*, 56, 554-577, 2009b.

658 Taylor, K. E., Stouffer, R. J., and Meehl, G. A.: AN OVERVIEW OF CMIP5 AND THE
659 EXPERIMENT DESIGN, *Bulletin of the American Meteorological Society*, 93, 485-
660 498, 2012.

661 Tjiputra, J. F., Olsen, A. R. E., Bopp, L., Lenton, A., Pfeil, B., Roy, T., Segschneider, J.,
662 Totterdell, I. A. N., and Heinze, C.: Long-term surface pCO₂trends from observations
663 and models, *Tellus B*, 66, 2014.

664 Tjiputra, J. F., Roelandt, C., Bentsen, M., Lawrence, D. M., Lorentzen, T., Schwinger, J.,
665 Seland, O., and Heinze, C.: Evaluation of the carbon cycle components in the
666 Norwegian Earth System Model (NorESM), *Geoscientific Model Development*, 6, 301-
667 325, 2013.

668 Uppstrom, L.R., 1974. BORON/CHLORINITY RATIO OF DEEP-SEA WATER FROM
669 PACIFIC OCEAN. *Deep-Sea Research*, 21(2): 161-162.

670 Vijayvargiya, A.: One-Way Analysis of Variance, *Journal of Validation Technology*, 15, 62-
671 63, 2009.

672 Watson, A. J., Schuster, U., Bakker, D. C. E., Bates, N. R., Corbiere, A., Gonzalez-Davila,
673 M., Friedrich, T., Hauck, J., Heinze, C., Johannessen, T., Körtzinger, A., Metzl, N.,
674 Olafsson, J., Olsen, A., Oschlies, A., Padin, X. A., Pfeil, B., Santana-Casiano, J. M.,
675 Steinhoff, T., Telszewski, M., Rios, A. F., Wallace, D. W. R., and Wanninkhof, R.:
676 Tracking the Variable North Atlantic Sink for Atmospheric CO₂, *Science*, 326, 1391-
677 1393, 2009.

678 Zeebe, R., E. and Wolf-Gladrow, D.: CO₂ in seawater, equilibrium, kinetics, isotopes,
679 Elsevier, Amsterdam, PAYS-BAS, 2001.
680
681

682 Table 1. Results and statistics of the regression analysis of fCO₂ (μatm) and pH_{insitu} versus
683 time. **Light-Boldgray** text indicates biomes where the results are not statistically significant
684 (95% confidence). No number is given if a biome does not have enough data to calculate the
685 trend in a given time period.

region	1981 – 2011				1991 – 2011			
	pH		fCO ₂		pH		fCO ₂	
	slope	rmse	slope	rmse	slope	rmse	slope	rmse
NP-SPSS	-0.0003±0.0005	0.041	1.209±0.17	16.2	0.0013±0.0005	0.038	0.748±0.22	16.1
NP-STSS	---	---	1.306±0.1509	10.5	-0.0010±0.0005	0.031	1.3754±0.130	8.9
NP-STPS	-0.0016±0.0002	0.020	1.5145±0.098	10.3	-0.0019±0.0002	0.018	1.527±0.124	9.9
WP-EQU	-0.0010±0.0002	0.016	1.5427±0.195	17.8	-0.0012±0.0002	0.015	1.597±0.273	17.3
EP-EQU	-0.0023±0.0003	0.023	2.9456±0.4136	28.2	-0.0026±0.0002	0.023	3.5133±0.5146	27.9
SP-STPS	-0.0019±0.0002	0.020	1.342±0.11	12.0	-0.0022±0.0003	0.020	1.125±0.186	12.3
NA-SPSS	---	---	1.18±0.2246	15.4	-0.0020±0.0004	0.028	1.11±0.2249	14.2
NA-STSS	---	---	1.78±0.2044	12.3	-0.0018±0.0003	0.015	1.798±0.2046	12.5
NA-STPS	---	---	1.426±0.1209	8.5	-0.0011±0.0002	0.012	1.4454±0.124	8.6
A-EQU	---	---	1.8662±0.3525	16.6	-0.0016±0.0003	0.014	1.8176±0.324	15.7
SA-STPS	---	---	1.06095±0.3724	16.7	-0.0011±0.0005	0.024	0.9982±0.374	17.0
IO-STPS	-0.0024±0.0004	0.023	1.494±0.254	13.6	-0.0027±0.0005	0.025	1.556±0.26	13.5
SO-STSS	-0.0006±0.0004	0.032	1.787±0.11	10.8	-0.0004±0.0004	0.032	1.8294±0.12	10.8
SO-SPSS	-0.0020±0.0002	0.020	1.440±0.1009	9.1	-0.0021±0.0002	0.020	1.465±0.11	9.0
SO-ICE	---	---	0.3470±0.3128	24.4	-0.0002±0.0004	0.029	0.235±0.343	24.3

686

687

688

689

690

691

692

693

694

695

696

697

698

699

700 Table 2. Decomposition of the fCO_2 - and pH_{insitu} trends into their major drivers. The units are
 701 $\mu atm yr^{-1}$ and pH -units yr^{-1} respectively.

Region	pH					fCO_2				
	theta	salinity	DIC	alkalinity	sum	theta	salinity	DIC	alkalinity	sum
NP-SPSS	-0.57	-0.15	3.18	-3.04	-0.58	0.52	0.14	-2.89	2.76	0.53
NP-STSS	-0.39	0.02	-0.89	-0.13	-1.39	0.38	-0.02	0.87	0.13	1.37
NP-STPS	1.15	-0.02	-1.68	0.04	-0.50	-1.19	0.02	1.73	-0.05	0.51
WP-EQU	-0.47	0.11	-0.87	0.14	-1.10	0.53	-0.12	0.97	-0.15	1.23
EP-EQU	0.51	-0.07	-2.99	0.13	-2.42	-0.63	0.08	3.68	-0.15	2.99
SP-STPS	2.28	-0.11	-3.02	0.04	-0.81	-2.47	0.12	3.28	-0.05	0.88
NA-SPSS	-0.02	0.17	-2.41	0.12	-2.13	0.01	-0.16	2.17	-0.11	1.91
NA-STSS	0.74	-0.07	-1.43	-0.11	-0.87	-0.72	0.07	1.40	0.10	0.85
NA-STPS	-1.20	-0.05	-0.10	-0.12	-1.47	1.29	0.05	0.11	0.13	1.57
A-EQU	-0.21	0.02	-1.33	-0.05	-1.56	0.24	-0.03	1.53	0.06	1.80
SA-STPS	-0.31	0.06	-1.55	-0.05	-1.85	0.34	-0.07	1.69	0.05	2.02
IO-STPS	0.80	-0.02	-3.23	0.06	-2.39	-0.79	0.02	3.22	-0.06	2.38
SO-STSS	-0.99	-0.08	2.02	-0.86	0.09	0.88	0.08	-1.81	0.77	-0.08
SO-SPSS	0.89	0.01	-3.09	0.53	-1.66	-0.83	-0.01	2.89	-0.50	1.56
SO-ICE	0.13	-0.01	-2.22	0.15	-1.95	-0.12	0.01	2.02	-0.13	1.78

702 Table 3. Decomposition of the 2001-2011 fCO_2 - and pH_{insitu} trends in the Southern Ocean into
 703 their major drivers. The units are $\mu atm yr^{-1}$ and pH -units yr^{-1} respectively.
 704

Region	pH						fCO_2					
	theta	salinity	DIC	alkalinity	sum	observed	theta	salinity	DIC	alkalinity	sum	observed
SO-STSS	-3.7	-0.79	8.46	-2.48	1.49	0.0032±0.0010	3.4	0.73	-7.78	2.28	-1.37	1.56±0.39
SO-SPSS	1.11	-0.07	-1.28	-0.05	-0.29	-0.0011±0.0006	-1.06	0.07	1.22	0.05	0.28	0.89±0.22
SO-ICE	-0.62	-0.05	1	-0.39	-0.06	0.0006±0.0009	0.59	0.05	-0.95	0.37	0.06	0.21±0.74

705
 706 **FigureFig. 1.** A map of the Fay and McKinley (2014) biomes which have (**aA**) a statistically
 707 significant pH trend in the period 1981-2011, and (**bB**) the biomes with a statistically
 708 significant pH trend in the period 1991-2011.

709
 710 **FigureFig. 2.** Long term fCO_2 - and pH trend (1981-2011) in the five Atlantic Ocean biomes.

711
 712 **FigureFig. 3.** Long term pH trend (1981-2011) in the five Pacific Ocean biomes.

713
 714 **FigureFig. 4.** Long term pH trend (1981-2011) in the Indian Ocean biome and the three
 715 Southern Ocean biomes.

716

717 | ~~Figure~~Fig. 5. Summary of the pH trends in all biomes. The error bars show the 1σ confidence
718 | interval.

719

720 | ~~Figure~~Fig. 6. Comparison between the observed pH trend in each biome (either 1981-2011 or
721 | 1991-2011) in black and the pH trends expected if the surface ocean $f\text{CO}_2$ changed equal to
722 | the atmosphere (blue) and expected for the observed ocean $f\text{CO}_2$ trends (red).

723

724 | ~~Fig. 7. The long term trends in pH from Fig. 2 decomposed into the contributions from SST,~~
725 | ~~SSS, alkalinity, and DIC. Also shown is the sum of the four contributions and the actual~~
726 | ~~observed trend. Note that the trend has been multiplied by 1000 for easier visualization.~~

727

728 | ~~Fig. 8. The long term trends in pH from Fig. 3 decomposed into the contributions from SST,~~
729 | ~~SSS, alkalinity, and DIC. Also shown is the sum of the four contributions and the actual~~
730 | ~~observed trend. Note that the trend has been multiplied by 1000 for easier visualization.~~

731

732 | ~~Fig. 9. The long term trends in pH from Fig. 4 decomposed into the contributions from SST,~~
733 | ~~SSS, alkalinity, and DIC. Also shown is the sum of the four contributions and the actual~~
734 | ~~observed trend. Note that the trend has been multiplied by 1000 for easier visualization.~~

735

736 | ~~Figure~~Fig. 107. The residual between the actual pH trends ~~in pH and $f\text{CO}_2$~~ and the sum of the
737 | four decomposition parts (SSS, SST, DIC, ALK). In gray is the residual for the observations,
738 | in black the residual for the sub-sampled model output, and in white the residual for the fully-
739 | sampled model output.

740

741 | ~~Figure 8. The long term trends in $f\text{CO}_2$ and pH from Figure 2 decomposed into the~~
742 | ~~contributions from SST, SSS, alkalinity, and DIC. Also shown is the sum of the four~~
743 | ~~contributions and the actual observed trend. Note that for pH the trend has been multiplied by~~
744 | ~~1000 for easier visualization.~~

745

746 | ~~Figure 9. The long term trends in $f\text{CO}_2$ and pH from Figure 3 decomposed into the~~
747 | ~~contributions from SST, SSS, alkalinity, and DIC. Also shown is the sum of the four~~
748 | ~~contributions and the actual observed trend. Note that for pH the trend has been multiplied by~~
749 | ~~1000 for easier visualization.~~

750

751

752

753

754

~~Figure 10. The long term trends in $f\text{CO}_2$ and pH from Figure 4 decomposed into the contributions from SST, SSS, alkalinity, and DIC. Also shown is the sum of the four contributions and the actual observed trend. Note that for pH the trend has been multiplied by 1000 for easier visualization.~~

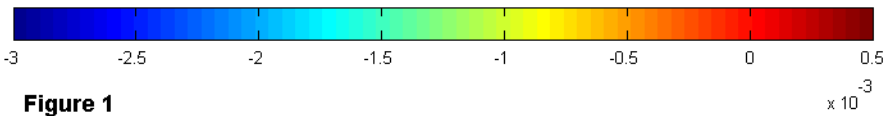
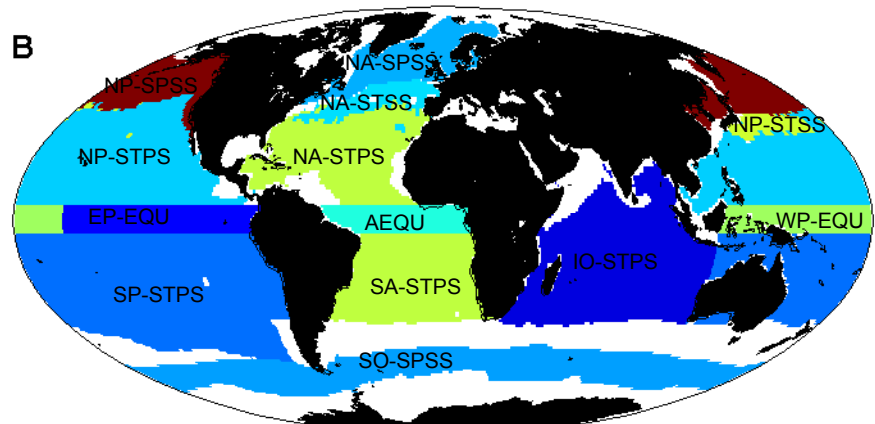
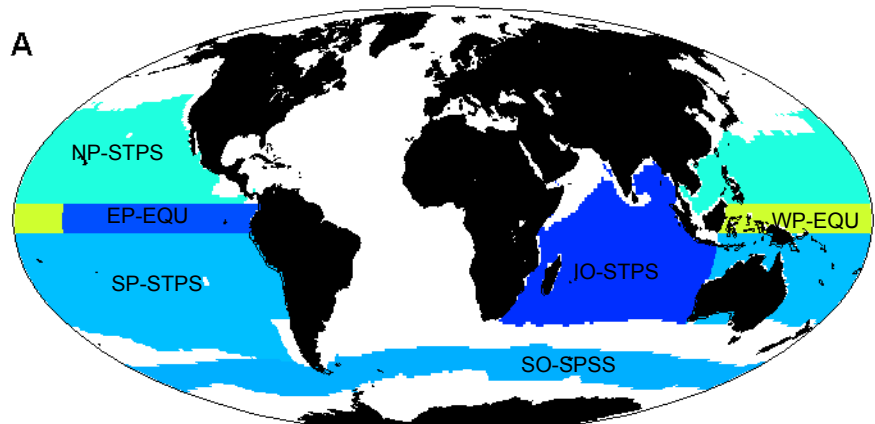


Figure 1

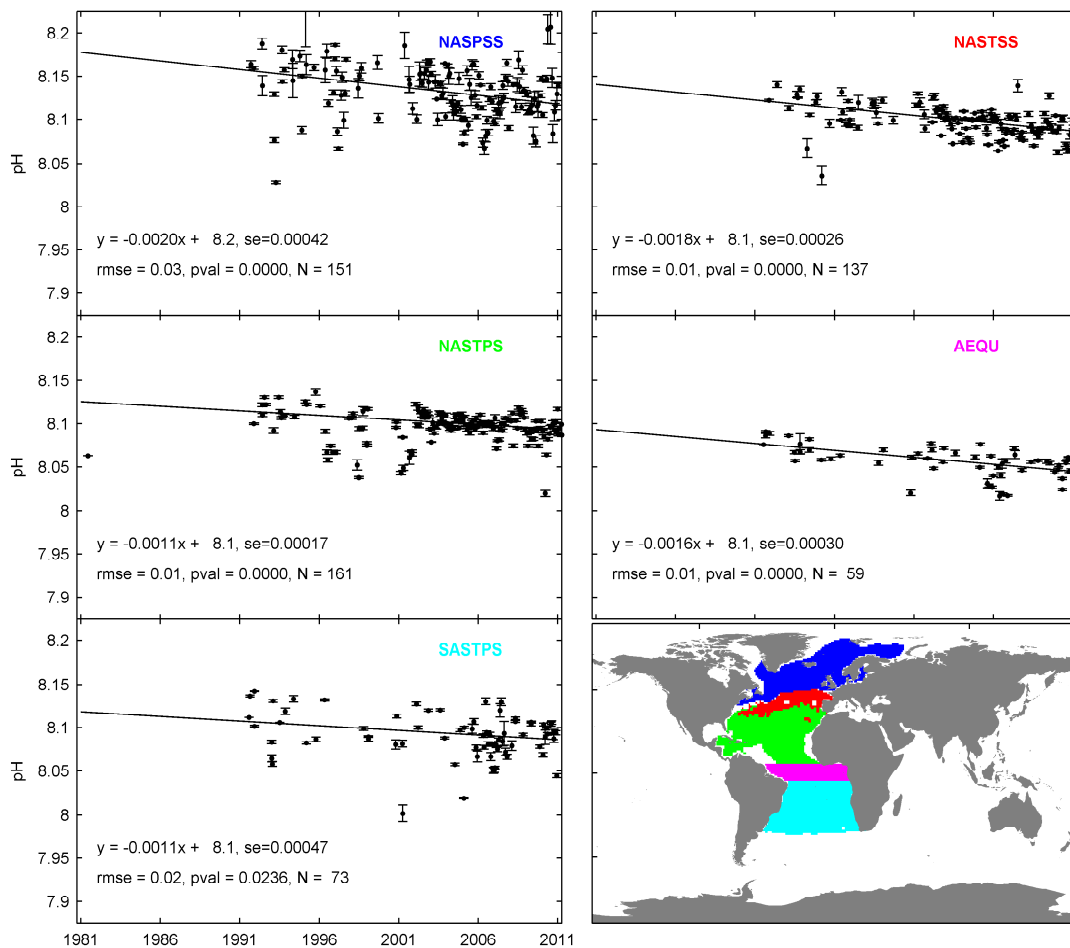


Figure 2

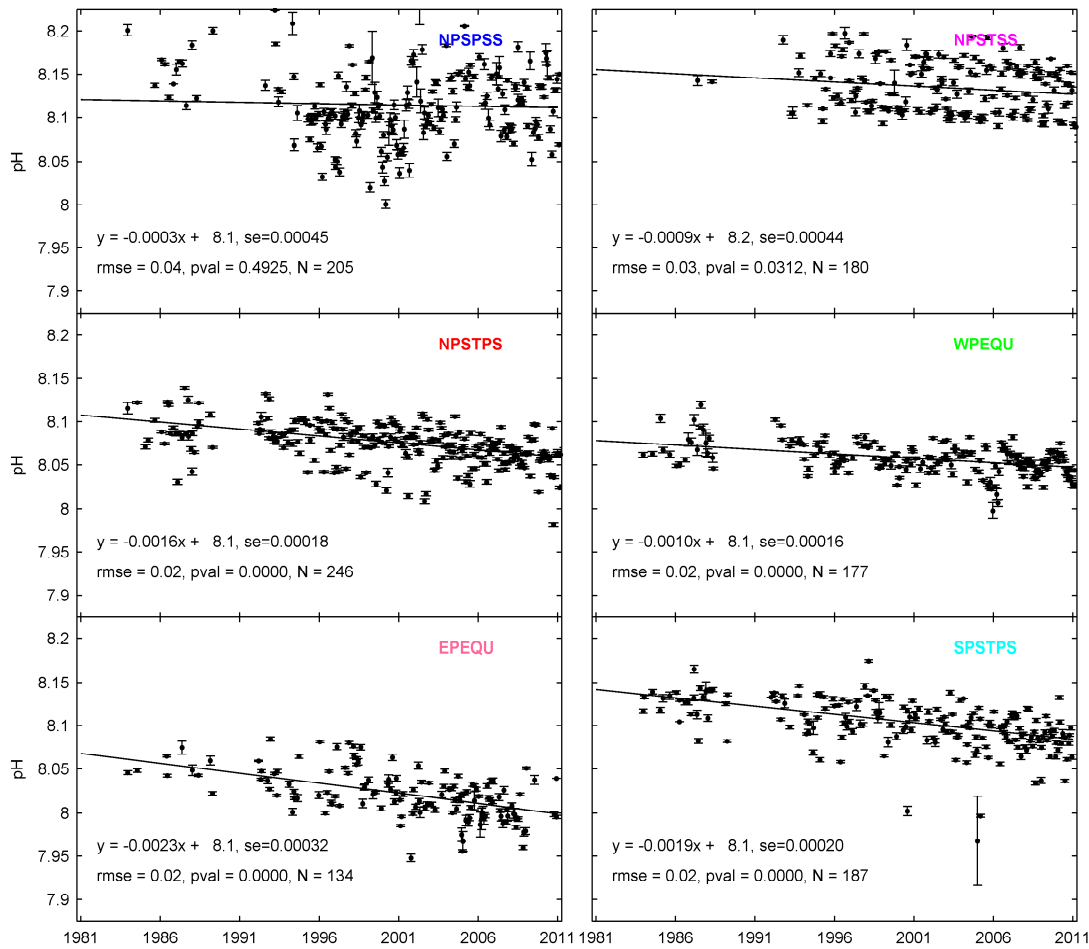
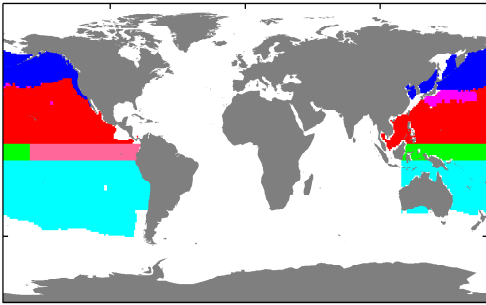


Figure 3

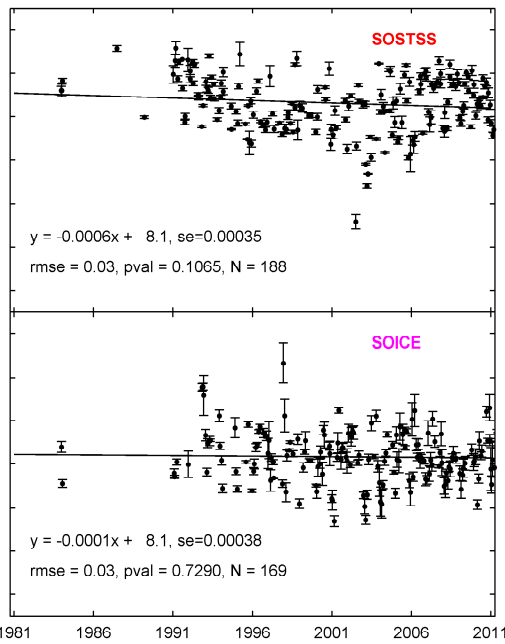
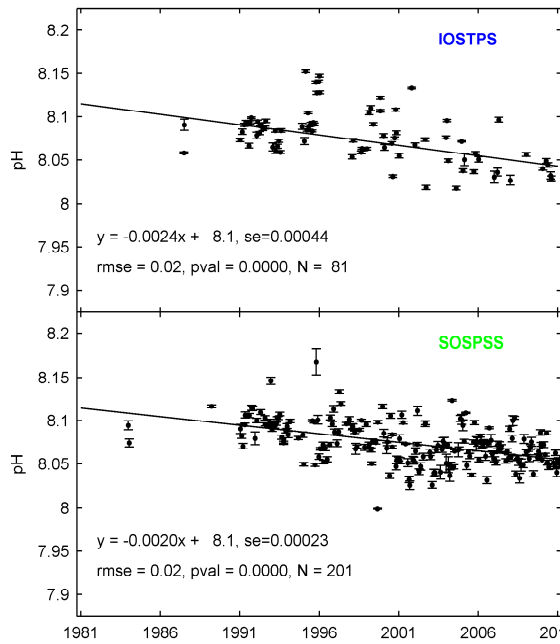
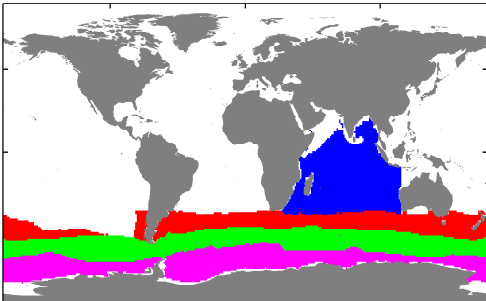


Figure 4

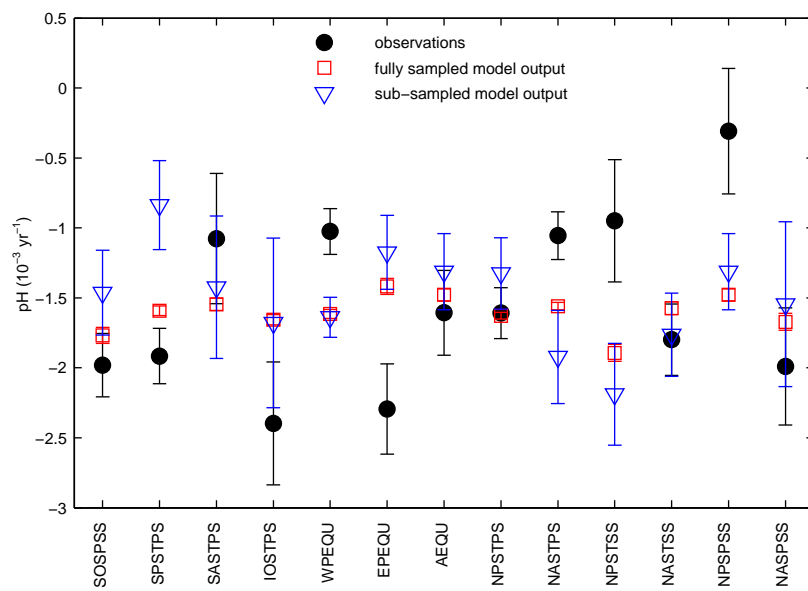


Figure 5

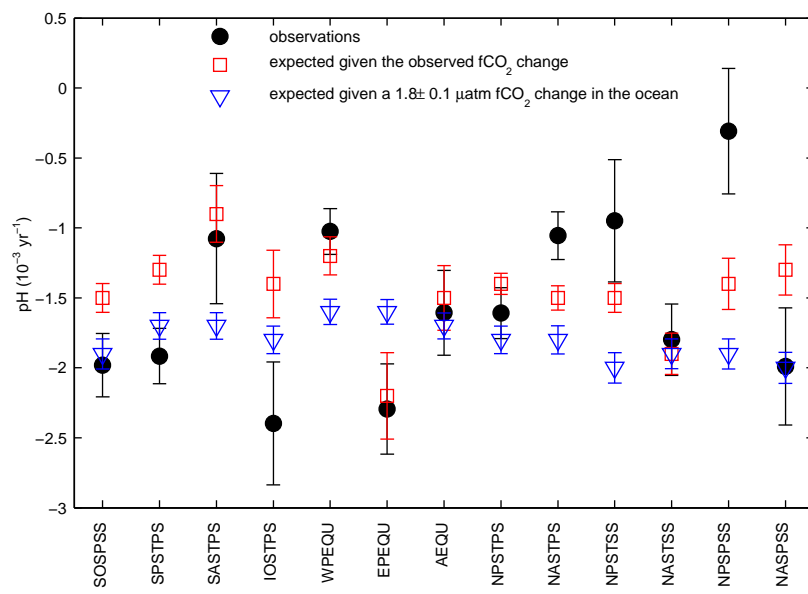


Figure 6

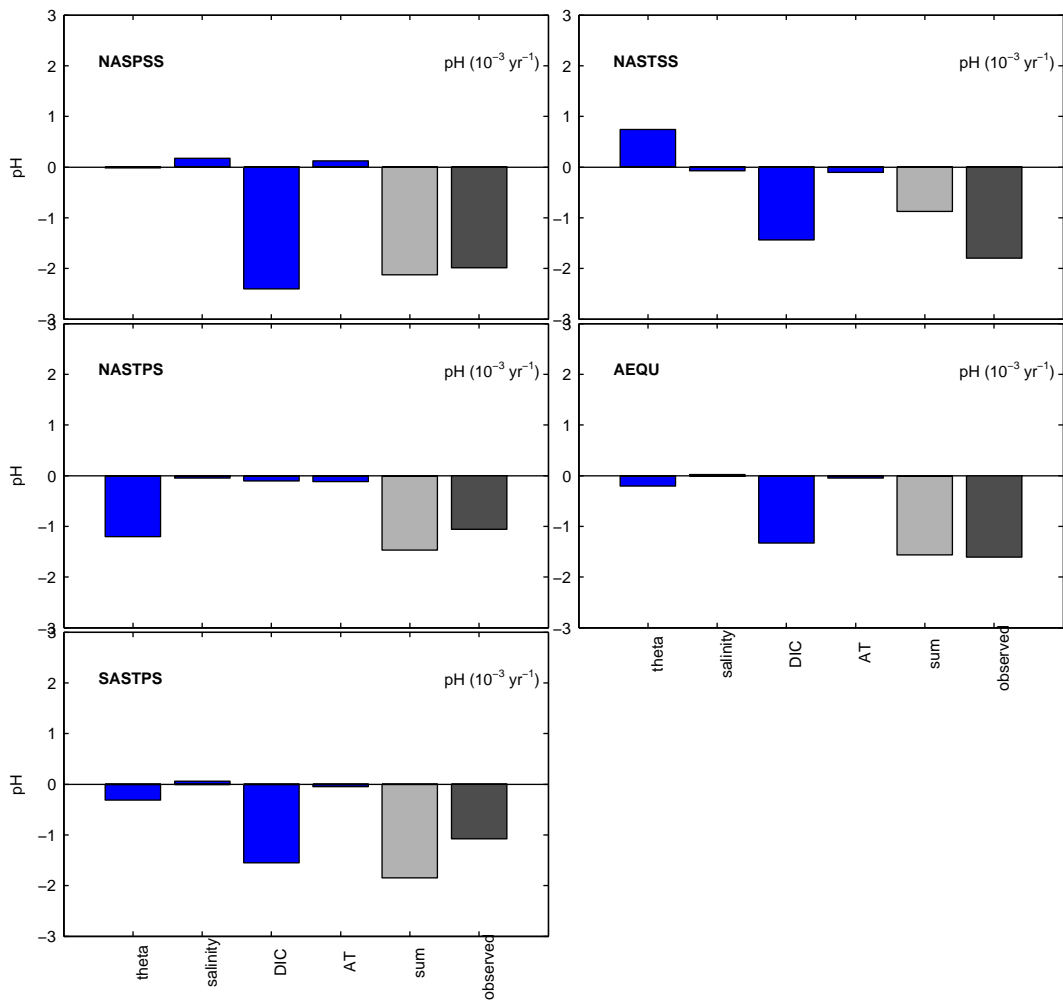


Figure 7

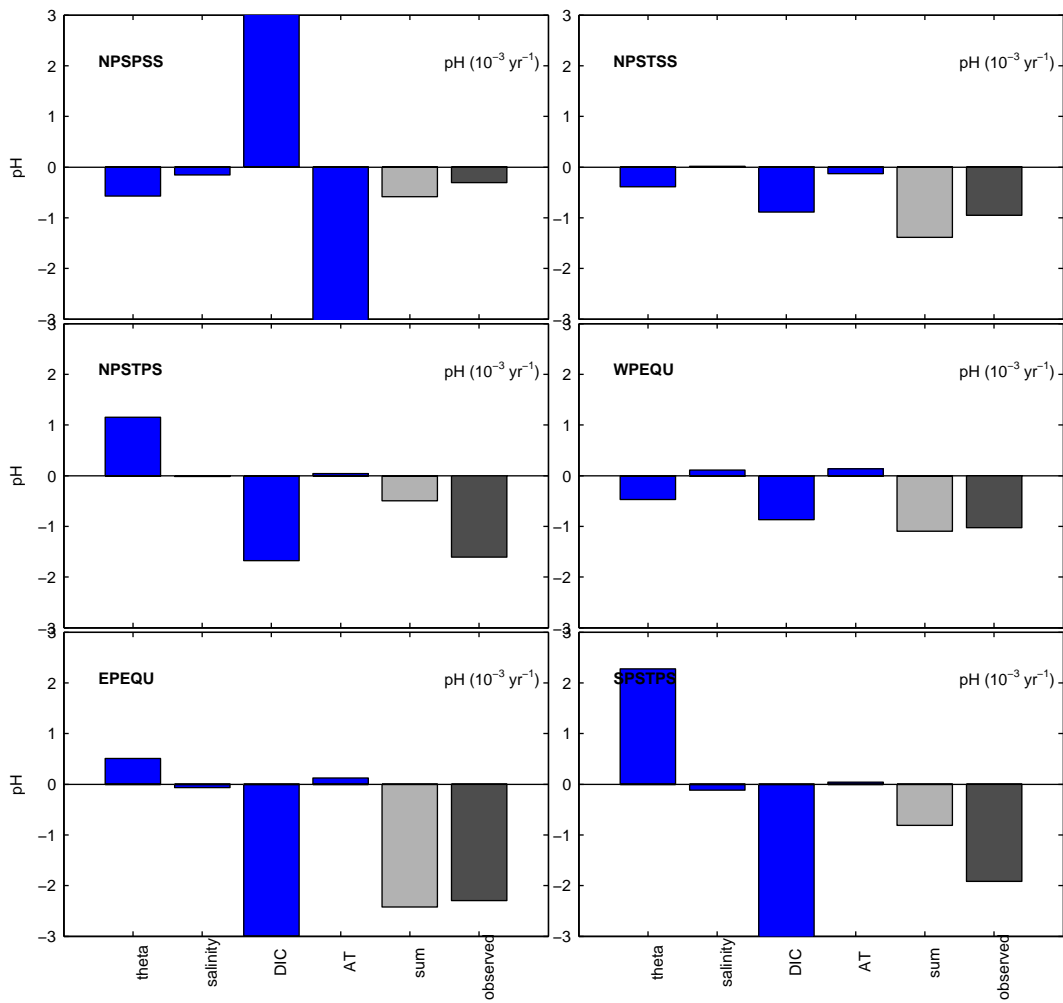


Figure 8

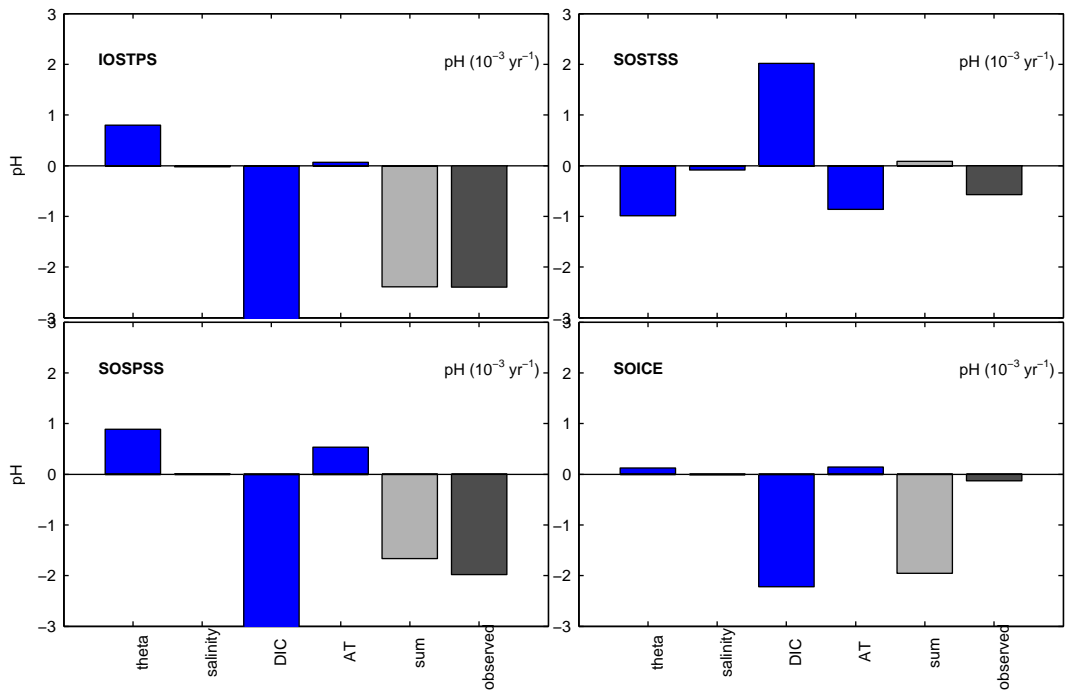


Figure 9

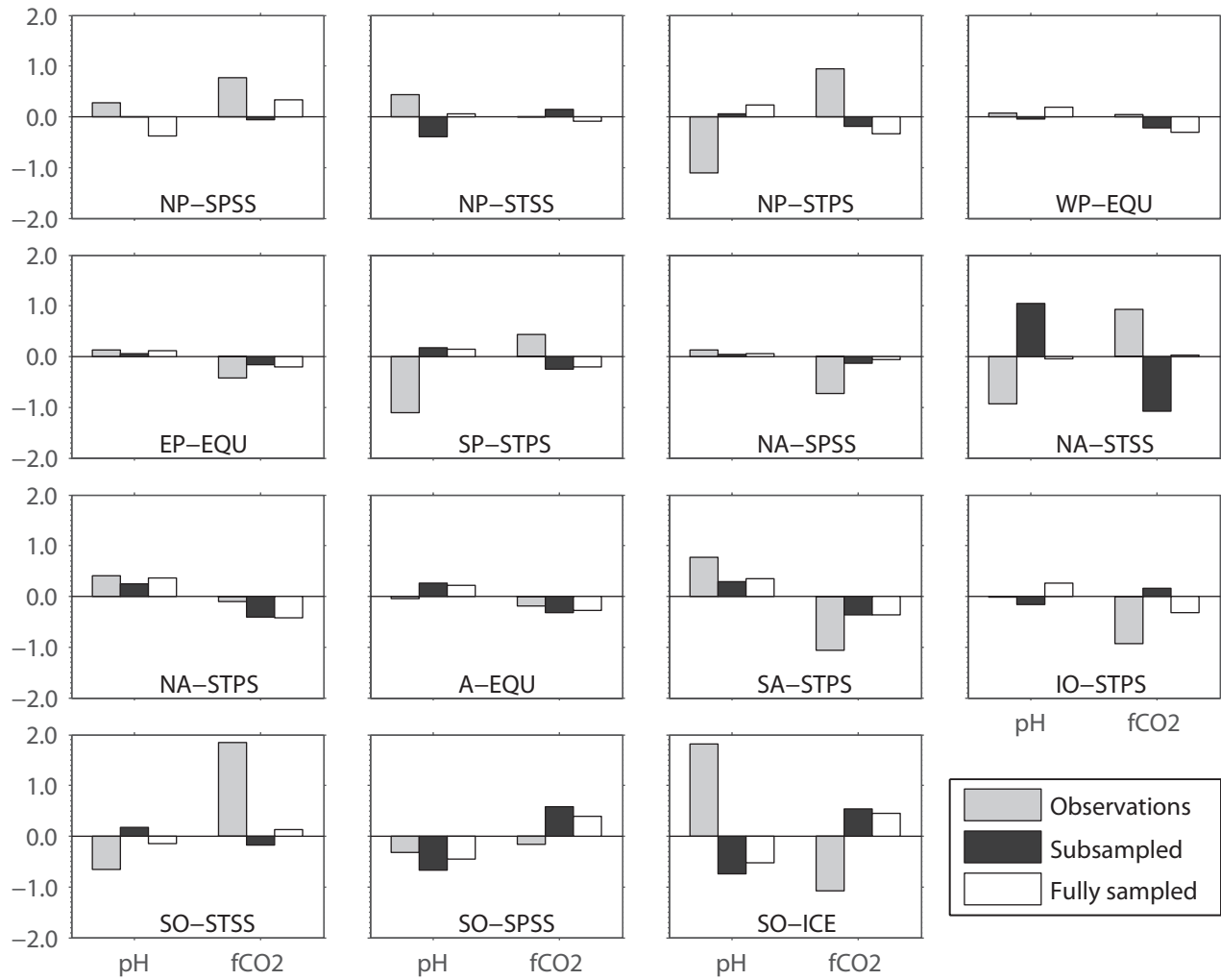


Figure 10